TISSUE ENGINEERING: Part A
Volume 24, Numbers 3 and 4, 2018

DOI: 10.1089/ten.tea.2016.0546

termis
Tissue Engineering
& Regenerative Medicine
International Society

ORIGINAL ARTICLE

Muscle-Secreted Factors Improve Anterior Cruciate Ligament Graft Healing: An *In Vitro* and *In Vivo* Analysis

Corina Adriana Ghebes, PhD,[1] Nathalie Groen, PhD,[2] Yau Chuk Cheuk, MPhil,[3,4] Sai Chuen Fu, PhD,[3,4] Hugo Machado Fernandes, PhD,[1,5] and Daniel B.F. Saris, MD, PhD[1,6]

One of the ligaments most often damaged during sports—the anterior cruciate ligament (ACL)—has poor healing capacity. On damage, reconstructive surgery is performed to restore the mechanical stability of the knee and to reduce the inflammatory milieu otherwise present in the joint. A return to normal activities, however, takes between 9 and 12 months. Thus, strategies capable of improving ACL graft healing are needed. Embryonic development of tendon and ligament (T/L) is regulated by a crosstalk between different cell types. We hypothesized that terminally differentiated skeletal-derived cells such as osteoblasts, chondrocytes, and myoblasts modulate T/L healing. Using an indirect coculture system, we discovered that myoblast-secreted signals—but not osteoblasts, chondrocytes, or stromal-secreted signals—are capable of upregulating classical T/L markers such as scleraxis and tenomodulin on human hamstring tendon-derived cells (hTC), which contribute to ACL graft healing. Transcriptome analysis showed that coculturing hTC with myoblasts led to an upregulation of extracellular matrix (ECM) genes and resulted in enhanced ECM deposition. *In vivo*, using a rat model of ACL reconstruction showed that conditioned media derived from human muscle tissue accelerated femoral tunnel closure, a key step for autograft integration. Collectively, these results indicate that muscle-secreted signals can be used to improve ACL graft healing in a clinical setting where muscle remnants are often discarded.

Keywords: ACL reconstruction, remnant muscle tissue, tendon graft healing

Introduction

The anterior cruciate ligament (ACL) is one of the most often damaged ligaments in the knee and, unfortunately, has very limited healing capacity, leaving surgical reconstruction as the only therapeutic option. More than 200,000 ACL reconstructions are performed annually in the United States alone.[1] A commonly used graft to replace the original ACL and restore its function is the hamstring tendon, which in comparison with the bone-patellar tendon-bone graft, gained popularity due to its accessibility, reduced pain, and lower morbidity rates.[2]

Following an ACL reconstruction, the mechanical stability of the knee joint is readily restored by means of fixation of the graft into the bone, while the necessary biological properties for long-term maintenance lag behind. In particular, vascularization, extracellular matrix (ECM) deposition, and integration of the soft tissue into the bone are key limiting steps in the regenerative process. Thus, improving at least one of these processes will contribute to ameliorating the recovery period and improving the patient's quality of life.

In a recent review, Schweitzer *et al.* described the mechanisms regulating musculoskeletal assembly in the vertebrate embryo emphasizing the reciprocal interactions between the forming tendons, muscle and cartilage tissue. Accordingly, the formation of complex tissues during embryonic development requires a continuous bidirectional communication between cells of different origins, such as

[1]MIRA Institute for Biomedical Technology and Technical Medicine, University of Twente, Enschede, The Netherlands.
[2]Department of Nephrology, Leiden University Medical Center, ZA Leiden, The Netherlands.
[3]Department of Orthopaedics and Traumatology, Faculty of Medicine, The Chinese University of Hong Kong, Prince of Wales of Hospital, Shatin, New Territories, Hong Kong, SAR, China.
[4]Lui Che Woo Institute of Innovative Medicine, Faculty of Medicine, The Chinese University of Hong Kong, Prince of Wales of Hospital, Shatin, New Territories, Hong Kong, SAR, China.
[5]Stem Cells and Drug Screening Lab, Center for Neuroscience and Cell Biology (CNC), University of Coimbra, Coimbra, Portugal.
[6]Department of Orthopaedics, University Medical Center Utrecht, Utrecht, The Netherlands.

muscle and tendon, or cartilage and tendon, to allow precise tissue assembly.[3]

Based on the abovementioned, we hypothesized that co-culturing human hamstring tendon-derived cells (hTC)—the cells present in the most commonly used autograft for ACL reconstruction—with myoblast-, osteoblast-, chondrocyte-, or stromal-derived cells could enhance the expression of tendon and ligament (T/L) markers and contribute to accelerating the healing process.

To test this, we used an *in vitro* indirect coculture system using transwell chambers, where we cultured human hTC in the presence of different cell types and investigated the expression of several T/L markers first by quantitative polymerase chain reaction (qPCR) and later using microarray analysis. Subsequently, we used an enzyme-linked immunosorbent assay (ELISA) to quantify the secretion of a panel of cytokines in our model system. Our results clearly indicate that coculturing hTC with myoblast or human muscle tissue (hMT)-derived condition media (CM) significantly increases the expression of T/L markers, ultimately leading to an increase in ECM deposition *in vitro*. Based on these findings, we used an *in vivo* rat model of ACL injury and, as expected, demonstrated that human muscle-CM accelerated femoral tunnel closure. A schematic representation of the experimental design is presented in Figure 1.

Materials and Methods

Cell culture

Samples of human hamstring tendon, cartilage harvested from tibial/femoral ends and bone marrow (BM) harvested from ilium were obtained from patients undergoing ACL reconstruction, knee replacement, or total hip arthroplasty, respectively. Cell isolation was carried out within 24 h after procurement as previously described.[4–6] The collection and anonymous use of the tissues and BM were approved and performed according to the medical ethical regulations and the guideline ''good use of redundant tissue for research'' of the Dutch Federation of Medical Research Societies (Ref. no. K13-46). Patients provided informed consent after being provided with a verbal explanation and an opportunity for questioning.

C2C12 (myoblast), MC3T3 (osteoblast), and ATDC5 (chondrocyte) mouse cell lines were obtained from American Type Culture Collection and cultured according to standard mammalian tissue culture protocols and sterile technique.[7–9]

Cells were expanded in basic media consisting of α-minimal essential media (Life Technologies), 10% fetal bovine serum (FBS; Lonza), 0.2 mM L-ascorbic acid 2-phosphate magnesium salt (Sigma), 100 U/mL penicillin

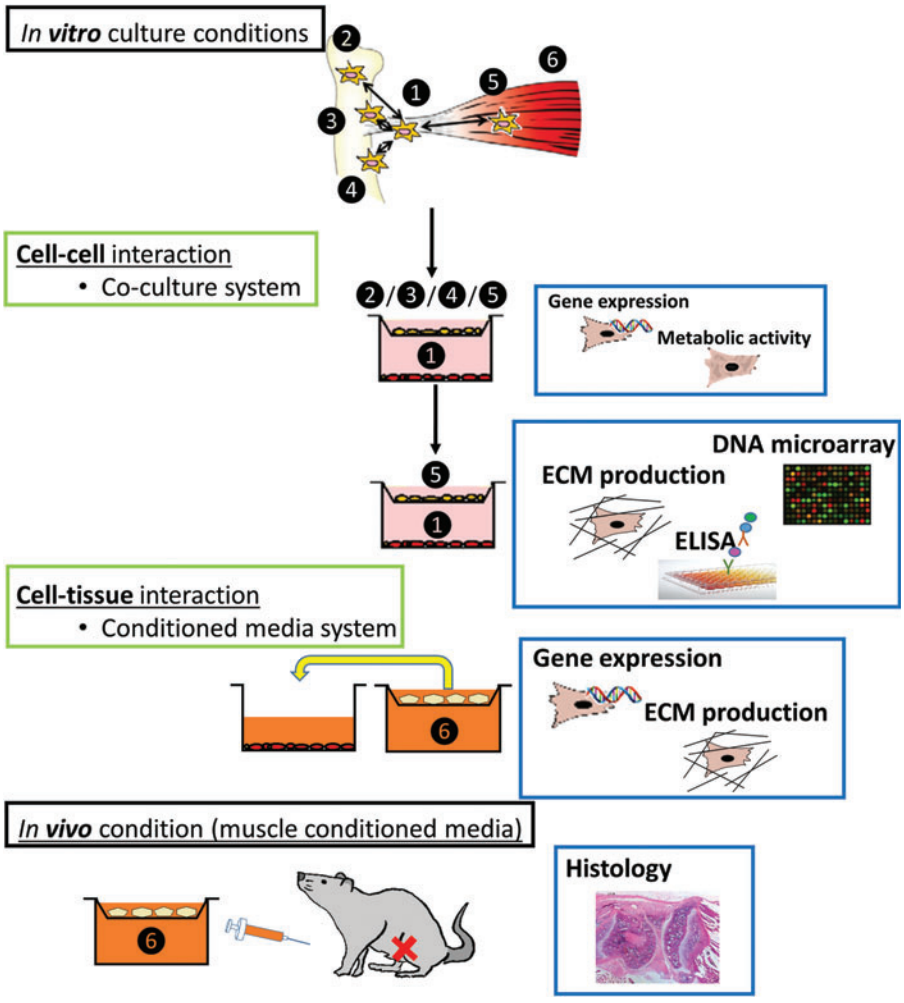

FIG. 1. Schematic overview of the experimental design. The number represents different types of cells or tissues used in the co-culture or condition media system: ❶ hTC, ❷ BM-hMSC, ❸ chondrocytes, ❹ osteoblasts, ❺ myoblasts, ❻ muscle tissue. BM-hMSCs, bone marrow-derived human mesenchymal stromal cells; hTC, hamstring tendon-derived cells. Color images available online at www.liebertpub.com/tea

(Gibco), and 100 mg/mL streptomycin (Gibco). Primary cells were never used beyond passage 4.

Indirect cell coculture system

An *in vitro* commercially available biocompartment culture system was used (1 μm pore size; Greiner Bio-One) to allow for an indirect exchange of humoral factors between the different cell types. In brief, hTC ($n=3$) were seeded onto the six-well outer tissue culture plate, while BM-derived human mesenchymal stromal cells (BM-hMSC) ($n=3$) or mouse myoblasts, chondrocytes and osteoblasts were seeded on the inner culture insert, at 100,000 cells per well/insert at a ratio of 1:1 and in triplicate. The cells were cultured separately for 1 day in basic media to allow an efficient cell attachment, after which the cell inserts were placed into the wells containing hTC and the media were changed to serum-reduced media (SRM) consisting of basic media with 1% FBS, rather than the abovementioned 10%. Media were refreshed every 3–4 days until the end of the experiment.

Conditioned media collection and use

hMT harvested from patients undergoing ACL reconstruction (remnant hamstring muscle) was washed in phosphate-buffered serum (PBS), minced into small pieces, and plated on a nontissue culture-treated six-well plate at ~2 g tissue/plate in SRM. CM, composed of SRM and muscle tissue secreted factors, was collected at day 3 and 7 and passed through a 100-μm filter to remove any remaining muscle tissue fibers. One day before the collection of hMT CM, hTC were plated at 100,000 cells/well on tissue culture six-well plates in triplicate in basic media. The next day, half of the media were replaced with hMT CM and the other half with SRM. The media were refreshed every 3 days until the end of the experiment.

Metabolic activity assessment

Metabolic activity was assessed at day 3 and 7 during the indirect cell coculture of hTC with BM-hMSCs or mouse myoblasts, chondrocytes, and osteoblasts. Cell inserts were removed from the indirect coculture system during the assessment of hTC metabolic activity. hTC were washed with PBS and incubated for 1 h with 10% (v/v) Presto Blue Cell Viability Reagent (Invitrogen) in SRM and absorbance was measured at 590 nm in triplicate.

RNA isolation and quantitative reverse transcription-polymerase chain reaction assessment

Total RNA was isolated from hTC using the NucleoSpin RNA II Isolation Kit (Macherey-Nagel), as per the manufacturer's instructions. RNA was collected in RNase-free water and a quantitative analysis was performed using spectrophotometry (NanoDrop). First-strand cDNA was synthesized from 800 ng total RNA/sample using iScript (BioRad) as per the manufacturer's instructions. qPCR was performed on a real-time PCR detection system (BioRad) using iQ SYBER Green Supermix (BioRad) for a panel of primers, described in Supplementary Table S1 (Supplementary Data are available online at www.liebertpub.com/tea), or using TaqMan Universal MasterMix for β2-microglobulin (*B2 M*) and scleraxis (*SCX*). Gene expression was normalized to the reference gene *B2 M*, and fold induction was calculated using the ΔΔCt method.

Microarray expression profiling

Gene expression profiling of two hTC donors cultured in triplicate in the absence or presence of mouse myoblasts was carried out using the Illumina microarray platform. cRNA was synthesized from 750 ng of total RNA using the Illumina TotalPrep RNA Amplification Kit (Ambion) as per the manufacturer's instruction, and cRNA quality was assessed using Bioanalyzer 2100 (Agilent). Next, cRNA was hybridized on Illumina HT-12 v4 expression beadchips overnight, after which the array was washed and blocked. Then, by adding streptavidin Cy-3, a fluorescent signal was developed and the arrays were scanned on an Illumina BeadArray reader and raw intensity values were background corrected in BeadStudio (Illumina). Further data processing and statistical testing were performed using R and Bioconductor statistical software.[10] The probe-level raw intensity values were quantile normalized and transformed using variance stabilization. A linear modeling approach with empirical Bayesian methods, as implemented in the Limma package,[11] was applied for differential expression analysis of the resulting probe-level expression values. *p*-Values were corrected for multiple testing using the Benjamini–Hochberg method.[12] Genes were considered differentially expressed between hTC cultured in the presence of myoblasts and hTC cultured alone, when a corrected *p*-value below 0.05 was reached with an absolute log2 fold change above 0.5. A Venn diagram (using Venny 2.1.0 BioinfoGP online tool) was used to represent the overlapping genes between the different conditions and donors. The differentially expressed genes (combining both up- and downregulated genes) overlapping between both donors were subjected to gene ontology (GO) analysis using DAVID bioinformatics resources.[13,14] The GO terms were considered significantly overrepresented when a Benjamini–Hochberg corrected *p*-value of 0.05 was reached.

Collagen content assessment

hTC were cocultured with myoblasts ($n=2$) or hMT CM ($n=1$) in triplicate for 29 days and media were refreshed every 3 days, as previously described. At day 29, the cells were fixed in 10% (v/v) buffered formalin for 15 min at room temperature and stained for collagen deposition using the Picrosirius red staining kit (Polyscience, Inc.), following the manufacturer's instructions. Images of the stained cells were acquired using a Nikon bright field microscope and quantification was performed using FIJI open source software. Images were converted to 8-bit and background subtracted using rolling ball radius function. The image was then converted into binary, and the area of Picrosirius red staining was selected and measured in total number of pixels.

Enzyme-linked immunosorbent assay

The supernatant of cocultured hTC ($n=2$) and myoblasts cultured on SRM for 3 days in triplicate was collected and immediately processed to assess the secretion of a panel of 23 cytokines and growth factors using ELISA plate array I for profiling 23 mouse cytokine proteins (BioCat), following the manufacturer's instructions.

ACL reconstruction in rat

The animal experiments were approved and performed in strict accordance with the recommendations and guidelines of the Animal Experimentation Ethics Committee in The Chinese University of Hong Kong (Ref. no. 15-166-MIS). ACL reconstruction was performed in 15 male Sprague Dawley rats (12 weeks old) on the right knee using ipsilateral flexor digitorum longus tendon, as previously described.[15] Under general anesthesia with ketamine and xylazine (75 and 25 mg/kg body weight, respectively), the flexor digitorum longus tendon (25 mm in length and 1 mm in diameter) was harvested by longitudinal medial incision of the right heel and the muscle tissue was removed from the graft. The knee joint capsule was opened, native ACL was excised, and the successful transection confirmed by a positive Lachman test. Tibia and femoral tunnels of 1.1 mm diameter, 9 mm and 6 mm in length were created from the footprints of the native ACL to the medial side of the tibia and the lateral femoral condyle. The tendon graft was inserted through both bone tunnels and the graft was fixed to the tibial periosteum first. Through a pulley system, a freely suspended weight was used to provide a constant tensioning force of 4 N to the graft during its fixation to the neighboring femoral periosteum. Finally, the fascia and other soft tissues were closed in layers. All animals were given 0.03 mg/kg body weight buprenorphine hydrochloride as analgesics and were allowed free cage activity after operation.

Postoperative intra-articular injection

hMT and tendon tissue harvested from the same patient undergoing ACL reconstruction (hTC 7) were washed in PBS, minced into small pieces, and plated in nontissue culture-treated plates separately at ~ 2 g per plate (Supplementary Fig. S1). Tissue samples were cultured in SRM for 3 days, after which CM was collected, strained through 100-μm filters, aliquoted, and stored at −80°C until use. SRM alone was collected and used as control. Five animals per condition were used. Intra-articular injection was performed on day 7, 14, 21, 28, and 35 postoperatively. The different CM were individually loaded into a 50-μL syringe with a 26G removable needle (Hamilton Company). Under general anesthesia with a mixture of isoflurane/O_2, with the knee flexed, the needle was inserted perpendicularly through patellar tendon to access the joint space, and 50 μL of treatment solution was slowly injected. The treatment regimen and necropsy time point were selected based on previous experience. To avoid injection in a swollen joint, intra-articular injection was performed from the first week, and as the drug clearance in the knee joint is fast, repeated injections were given on a weekly basis up to the 6th week postoperation, when improvement in tendon graft healing was previously observed.[16]

Histological analysis

At 6 weeks postoperation, the rats were euthanized with an overdose of pentobarbital. The harvested knee joints were fixed in 10% (v/v) buffered formalin, decalcified in 9% formic acid for 5 weeks, and embedded in paraffin. Five-micrometer-thick paraffin sections along the sagittal plane of the knee were collected. From each animal, two or three sections were chosen for histological examination of femoral tunnels, intra-articular graft midsubstance, and tibial tunnels.[17] Sections from the epiphyseal region were chosen for comparison of graft healing inside tunnels. H&E-stained sections were examined under bright field light (Leica Microsystems).

Statistical analysis

Statistical analysis was performed using GraphPad Prism 6 software. Two-way ANOVA and a Tukey *post hoc* test or unpaired Student's *t*-test were used to compare the different conditions. A $p \leq 0.05$ indicates a statistically significant difference. Results are shown as mean ± standard deviation.

Results

Upregulation of tendon/ligament markers in hTC cocultured with myoblasts

Indirect coculture of hTC with BM-hMSCs, myoblasts, osteoblasts, and chondrocytes resulted in differential expression of lineage-specific markers compared with the untreated control. Although coculture of hTC with BM-hMSCs and osteoblasts did not change the expression of T/L genes—neither of the genes related with chondrogenesis and osteogenesis—it was interesting to observe the effect of coculturing hTC with myoblasts and chondrocytes. Coculturing hTC with chondrocytes significantly increased the expression of chondrogenic (28.6 ± 28.5- and 3.7 ± 3.6-fold increase vs. control for cartilage oligomeric matrix protein [*COMP*] and aggrecan [*ACAN*], respectively) and osteogenic marker (12.6 ± 18.77-fold increase vs. control for alkaline phosphatase). It is notable that coculturing hTC with myoblasts led to a statistically significant increase in the expression of *SCX* (5.5 ± 4.4-fold vs. control)—the master transcription factor involved in T/L specification. Moreover, tenomodulin (*TNMD*)—a well-recognized T/L lineage marker—was also upregulated solely on hTC exposed to myoblasts (8.1 ± 1.7-fold) (Fig. 2 and Supplementary Fig. S2). Furthermore, T/L-related genes such *COL1A1* (2.8 ± 2-fold), *TNC* (2.4 ± 1.6-fold), and *COMP* (8.6 ± 6-fold) were also increased in hTC exposed to myoblasts but did not achieve a statistically significant difference.

No visual morphological changes were observed in hTC between the different coculture conditions at day 7 (data not shown).

hTC metabolic activity is limited, affected by the coculture system

Coculture of hTC with BM-hMSCs, myoblasts, osteoblasts, and chondrocytes resulted in no statistically significant differences in hTC metabolic activity, with the exception of one donor where myoblasts significantly increased the metabolic activity of hTC at both time points and chondrocytes significantly decreased the metabolic activity in a different donor at day 7 (Supplementary Fig. S3).

Coculture of hTC with chondrocytes does not increase the expression of T/L markers

Based on the abovementioned results, we decided to validate our findings on human-derived cells. To that end,

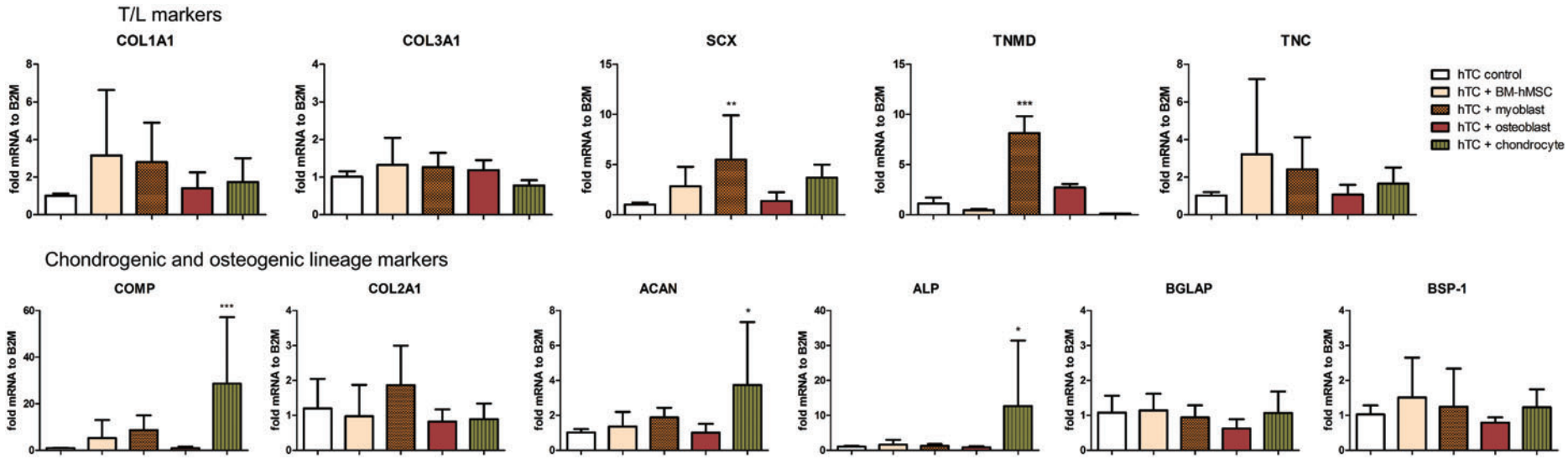

FIG. 2. Gene expression of tendon-/cartilage- and bone-related markers in hTC when cultured in the presence of BM-hMSCs, myoblasts (C2C12), osteoblasts (MC3T3), or chondrocytes (ATDC5) for 7 days in 1% fetal bovine serum media. The graphs represent the average in gene expression over 3 hTC donors. Statistically significant differences were found with ***$p < 0.001$, **$p < 0.01$, and *$p < 0.05$. Color images available online at www.liebertpub.com/tea

we exposed primary isolated human hTC to primary isolated human chondrocytes and investigated the expression of a set of T/L- and cartilage-related genes. With the exception of *TNMD*, which was downregulated, coculturing human primary hTC with human primary chondrocytes did not change the expression of T/L markers compared with the control (Supplementary Fig. S4). Based on these findings, we decided to focus on the role of myoblasts on hTC.

Genome-wide analysis of gene expression in hTC exposed to myoblasts

To unravel the molecular players governing the interaction between hTC and myoblasts, we performed a genome-wide gene expression analysis to identify which genes were differentially regulated on hTC (from two different donors) exposed to myoblasts compared with the control. Transcriptional profiling revealed a total of 60 genes upregulated and 90 genes downregulated in hTC cultured in the presence of myoblasts versus control (Fig. 3a). The top 20 up- and downregulated genes and respective log2 fold change are presented in Figure 3b, while the complete list comprising gene name, log2 fold change, and gene function and location can be found in Supplementary Table S2. A brief analysis of the top 20 genes reveals an enrichment in genes involved in ECM modulation, such as *COMP*; tissue inhibitor of metalloproteinases 3 (*TIMP3*); collagen type XI alpha 1 (*COL11A1*); retinoic acid receptor responder 2 (*RARRES2*); polypeptide N-acetylgalactosaminyltransferase 1 (*GALNT1*); stimulator of chondrogenesis 1 (*SCRG1*); fibronectin type III domain containing 1 (*FNDC1*); chitinase 3 like 1 (*CHI3 L1*); C-X-C motif chemokine ligand 12 (*CXCL12*); platelet-derived growth factor receptor like (*PDGFRL*); and complement C1r subcomponent (*C1R*) (Fig. 3b, pattern-containing bars). In addition, using the identified up- and downregulated genes (60 + 90) and GO enrichment analysis, we found significantly enriched GO categories in biological adhesion (GO: 0022610, fold enrichment 2.9, p-value = 0.05); response to wounding (GO: 0009611, fold enrichment 3.6, p-value = 0.03); proteinaceous ECM (GO: 0005578, fold enrichment 4.4, p-value = 0.004); extracellular region part (GO: 0044421, fold enrichment 2.7, p-value = 0.003); ECM (GO: 0031012, fold enrichment 4.8, p-value = 0.0006); and extracellular region (GO: 0005576, fold enrichment 2.4, p-value = 0.000008) (Fig. 3c). This analysis clearly demonstrates the influence myoblasts exert on the modulation of ECM molecules in hTC. In addition, we found that within these ECM modulators, several genes were involved in the formation and remodeling of cartilage ECM, such as *COMP*, *COL 11A1*, *TIMP3*, *SCRG1*, or *CHI3 L1* (Fig. 3d, orange circles). Furthermore, GO enrichment analysis revealed that, although not significant, a large number of genes were involved in the regulation of cell migration, motion, and locomotion, such as laminin subunit alpha 4 (*LAMA4*); podoplanin (*PDPN*); ectonucleotide pyrophosphatase/phosphodiesterase 2 (*ENPP2*); platelet-derived growth factor receptor alpha (*PDGFRA*); thrombospondin 1 (*THBS1*); adenosine A1 receptor (*ADORA1*); tropomyosin 1 (*TPM1*); *CXCL12*; LIM zinc finger domain containing 2 (*LIMS2*); annexin A2 (*ANXA2*); tensin 3 (*TNS3*); *RARRES2*; actin; and alpha 2 smooth muscle aorta (*ACTA2*) (Fig. 3d, dark green circles). Finally, we analyzed the location of the identified gene functions and found that the majority of the gene functions were located within the cytoplasm (34%), followed by plasma membrane (23%), extracellular space (18%), and nucleus (10%) (Fig. 3e). Gene function analysis showed an enrichment in genes involved in enzyme (17%), while a small percentage of genes were involved in kinase, transmembrane receptor, peptidase, and transcription regulator (each 5%), or phosphatase (3%) and cytokine and G-protein-coupled receptor (2%). The remaining genes showed enrichment in other classes of genes (52%) (Fig. 3f).

Analysis of cytokine panel secreted by myoblasts cocultured with hTC

To identify which factors secreted by myoblasts may be responsible for the effects observed on hTC, we performed a protein array study in which we analyzed a panel of cytokines and growth factors released in the culture media during indirect coculture of myoblasts with hTC. Our results showed that, compared with the control (hTC alone), coculture with myoblasts upregulated the expression of monocyte chemoattractant protein-1 (MCP-1) 7.4-fold, vascular endothelial growth factor (VEGF) 1.4-fold, interleukin 6 (IL-6) 1.8-fold, and Rantes 1.7-fold (Fig. 4).

hTC exposed to hMT CM upregulate T/L genes

To translate our findings into a potential therapy for T/L healing, we decided to analyze whether hTC responded similarly when exposed to soluble factors obtained from hMT. To do so, we exposed hTC to hMT CM from three different donors for 7 days. In line with the results obtained for myoblasts, our results showed a statistically significant upregulation for *TNMD* (40 ± 40-fold), *TNC* (1.5 ± 0.3-fold), and *COMP* (2 ± 0.7-fold) between hMT CM-treated cells versus control (Fig. 5 and Supplementary Fig. S5).

Myoblast indirect coculture and hMT CM enhance collagen production

Given the effects observed in the expression of ECM-related genes on indirect coculture of hTC with myoblasts and hMT CM, we proceeded to quantify the amount of collagen produced by hTC exposed to the respective condition for 29 days. We found that, compared with the control, hTC exposed to myoblasts significantly increased the production of collagen (1.7-fold for hTC1 and 2.2-fold for hTC2; Fig. 6a, b, d, e, and g, h), while the addition of hMT CM resulted in a 3.3-fold increase for hTC6 (Fig. 6c, f, i). Based on these results, we decided to test the effect of hMT CM in a rat model of ACL reconstruction.

Treatment of hMT CM improved healing after ACL reconstruction

A rat ACL reconstruction model was used to test the effects of hMT CM. Tendon tissue CM were used as control for the *in vivo* study. At 6 weeks postoperation, healing responses were evident in all ACL reconstructed rat knees, with respect to bone tunnel healing, bone-to-graft incorporation, and tendon graft remodeling (Fig. 7). The presence of Sharpey's fiber and/or fibrocartilage interface (Fig. 7d–i) was observed at the graft incorporation to surrounding bone in both femoral and tibial tunnels and in all groups. In

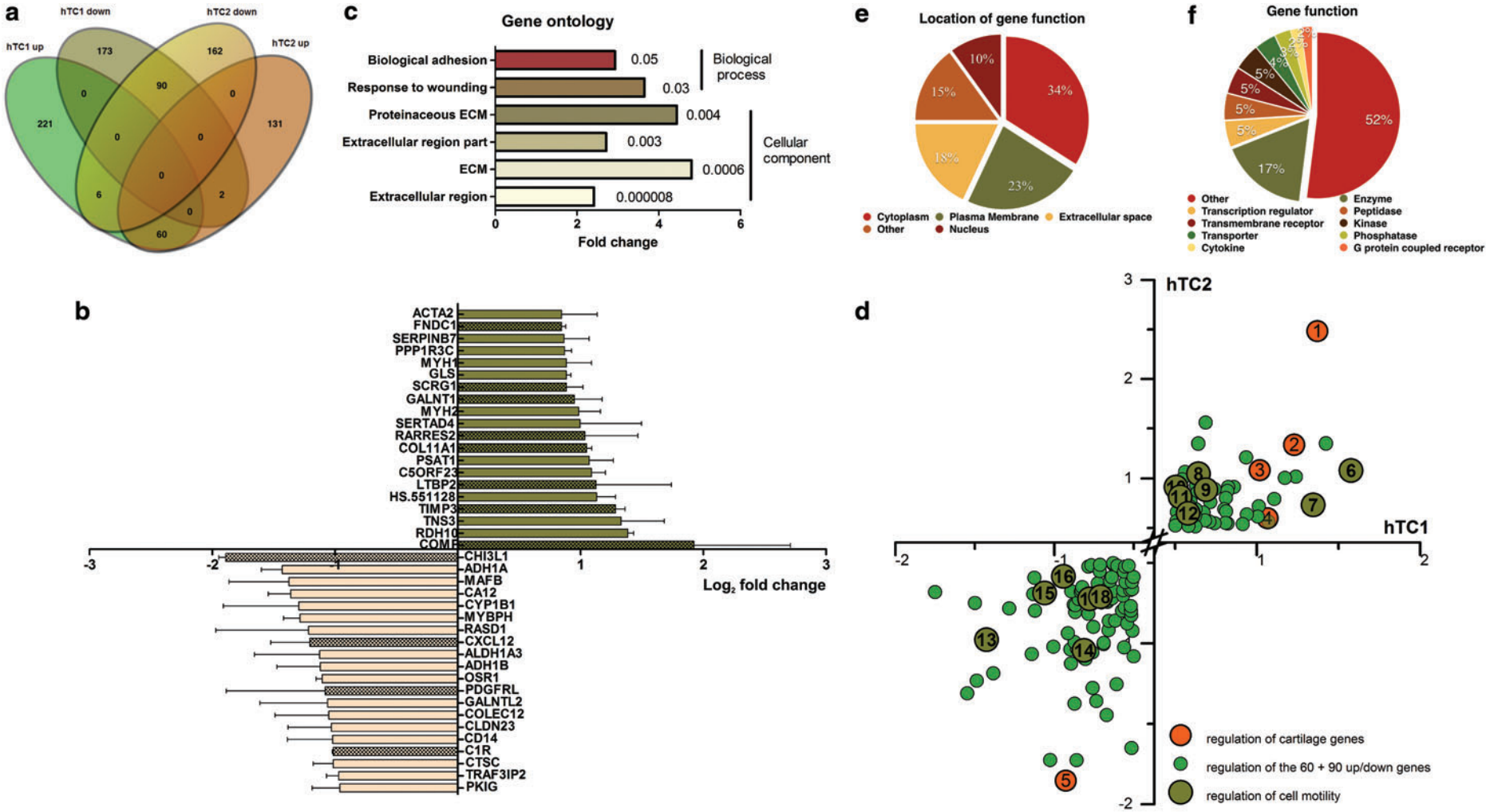

FIG. 3. Genome-wide microarray and GO analysis of differentially expressed probe sets. **(a)** Venn diagram of differentially expressed genes. The number of significant up- and downregulated genes in hTC1 and hTC2 and their intersection, indicating the number of common and individually regulated genes. Differentially expressed genes were identified by pairwise comparison analysis of hTC+myoblasts and hTC alone. **(b)** Map of the top 20 up- and downregulated genes, including the *p*-values. Pattern graphs represent genes involved in ECM remodeling. **(c)** GO analysis of all common differentially expressed genes and the identified significantly enriched biological process and cellular component GO clusters. **(d)** hTC1 versus hTC2 plot of log2 fold change of the differentially expressed genes. positive log2 fold change defines positive expression of genes in hTC indirectly cocultured with myoblasts and reverse for negative log2 fold change. *Orange circles* represent genes that regulate cartilage [(1) COMP, (2) TIMP3, (3) COL11A1, (4) CHRDL2, (5) CHI3 L1, dark *green circles* represent genes that regulate cell motility (6) TNS3, (7) RARRES2, (8) ACTA2, (9) ANXA2, (10) TPM1 (11), LIMS2, (12) THBS1, (13) CXCL12, (14) ENPP2, (15) ADORA1, (16) LAMA4, (17) PDPN, (18) PDGFRA], while small *green circles* represent the rest of the 60+90 commonly expressed genes. **(e)** Pie diagram representing the location of gene function. **(f)** Pie diagram representing gene function. ACTA2, alpha 2 smooth muscle aorta; ADORA1, adenosine A1 receptor; ANXA2, annexin A2; CHI3 L1, chitinase 3 like 1; COL11A1, collagen type XI alpha 1; COMP, cartilage oligomeric matrix protein; CXCL12, C-X-C motif chemokine ligand 12; ECM, extracellular matrix; ENPP2, ectonucleotide pyrophosphatase/phosphodiesterase 2; GO, gene ontology; LAMA4, laminin subunit alpha 4; LIMS2, LIM zinc finger domain containing 2; PDGFRA, platelet-derived growth factor receptor alpha; PDPN, podoplanin; RARRES2, retinoic acid receptor responder 2; TNS3, THBS1, thrombospondin 1; TIMP3, tissue inhibitor of metalloproteinases 3; tensin 3; TPM1, tropomyosin 1. Color images available online at www.liebertpub.com/tea

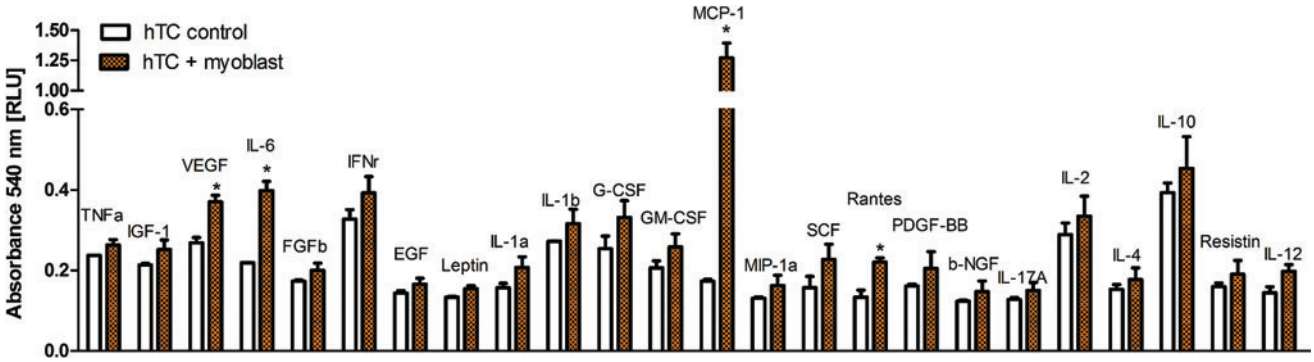

FIG. 4. Protein array study showing cytokines and growth factors produced by mouse myoblast cell line when cocultured with hTC1 and hTC2. The values are shown as the average over the two hTC donors and represented as relative light unit. Mouse myoblasts have been shown to produce VEGF, IL-6, MCP-1, and Rantes. Statistically significant differences were found with $*p < 0.05$. IL, interleukin; MCP-1, monocyte chemoattractant protein-1; VEGF, vascular endothelial growth factor. Color images available online at www.liebertpub.com/tea

addition, the cellularity in the tendon graft at the intra-articular portion was high in all groups, whereas the degree of cell infiltration in bone tunnels varied between different groups (Fig. 7j–l). Bone tunnel closure did not show any significant differences in tibial bone tunnel closure between groups; however, significant femoral bone tunnel closure was observed in hMT CM group (four out of five samples) (Fig. 7c, f) compared with the basic media group (one out of five samples) (Fig. 7a, d) and tendon CM group (one out of five samples) (Fig. 7b, e).

Discussion

Intra-articular healing and remodeling of tendon grafts, following an ACL reconstruction, have been described in the literature as a complex and long-term process, which delays the time for patients to return to work and sport activities.[18,19] To improve the healing process and the integration of the tendon graft into the new environmental conditions, we approached the remodeling process by engaging the use of cellular crosstalk known to trigger signaling cascades beneficial in tissue remodeling. Inspired by embryonic development of T/L, where tendon cells experience behavioral changes as result of interaction with surrounding tissue cells, we explored, in a simplified 2D *in vitro* model, the effects of surrounding mature tissue cells, such as myoblasts, chondrocytes, osteoblasts, or BM-hMSC on the expression of a panel of ECM, and differentiation genes in tendon cells and on the metabolic activity of hTC. We found that myoblasts and chondrocytes modulated tendon cellular responses, resulting in an increased expression of tendon- and cartilage-related markers, but have limited influence on hTC metabolic activity. The expression of *SCX* in hTC exposed to myoblasts was accompanied by expression of *TNMD*. This regulatory effect exerted by skeletal muscle cells on tendon cells by exchange of paracrine factors has been previously reported to occur during tendon development, where the expression of *SCX* and *TNMD* was described to be dependent on muscle signals.[20,21] To better understand the role that myoblasts play in modulating tendon cell commitment, we performed a genome-wide analysis on tendon cells, using the same experimental and donor setting. We found that a large majority of differentially expressed genes were involved in ECM modulation. Since it is known that ECM remodeling plays a key role in restoring the biology and function of T/L during the healing process, and since myoblasts play a key role in tissue contraction and organ fibrosis during wound healing,[22,23] our findings suggest that in a simplified 2D environment, with no tensile forces, the chemokines released by myoblasts were enough to affect matrix synthesis and turnover. Further analysis identified that some of the differentially expressed ECM genes—*COMP*, *COL11A1*, *TIMP3*, *SCRG1*, *CHI3 L1*, or *CHRDL2* are known to be involved in cartilage matrix remodeling,[24–29] suggesting an important role in guiding tendon–bone interface regeneration. Other regulated genes were found to be involved in cell migration and motion, such as *TNS3*, *RARRES2*, *ACTA2*, *ANXA2*, *TPM1*, *LIMS2*, *THBS1*, *CXCL12*, *ENPP2*, *ADORA1*, *LAMA4*, *PDPN*, and *PDGFRA*,[30–42] suggesting an important role for cell migration on the repopulation of the tendon graft, while influencing revascularization and tendon–bone closure. To elucidate the molecular signals exchanged between myoblasts and hTC, we analyzed a panel of cytokines and identified MCP-1, VEGF, Rantes, and IL-6 as being secreted by myoblasts during indirect coculture with both hTC donors. We propose two explanations that relate the expression of the identified cytokines to the regulation of genes. One explanation is the fact that MCP-1, VEGF, and Rantes are known chemotactic cytokines,[43–45] which may explain the regulation of a large number of genes involved in cell migration and motion. Second, Rantes and IL-6 are also known as inflammatory cytokines, which may explain the regulation of genes involved in GO category response to wounding. The regulation of chemotactic and inflammatory cytokines can attract at first the migration of inflammatory cells, which can induce a catabolic phase in which they release a variety of matrix metalloproteases,[46] essential for initiation of ECM remodeling. Next, other types of cells, such as macrophages, can be also attracted and initiate ECM deposition by their release of different growth factors. Future work should focus on the thorough analysis of the proteome using more donors, ideal human-derived terminally differentiated skeletal cells, and techniques capable of identifying a higher number of proteins such as mass spectrometry.

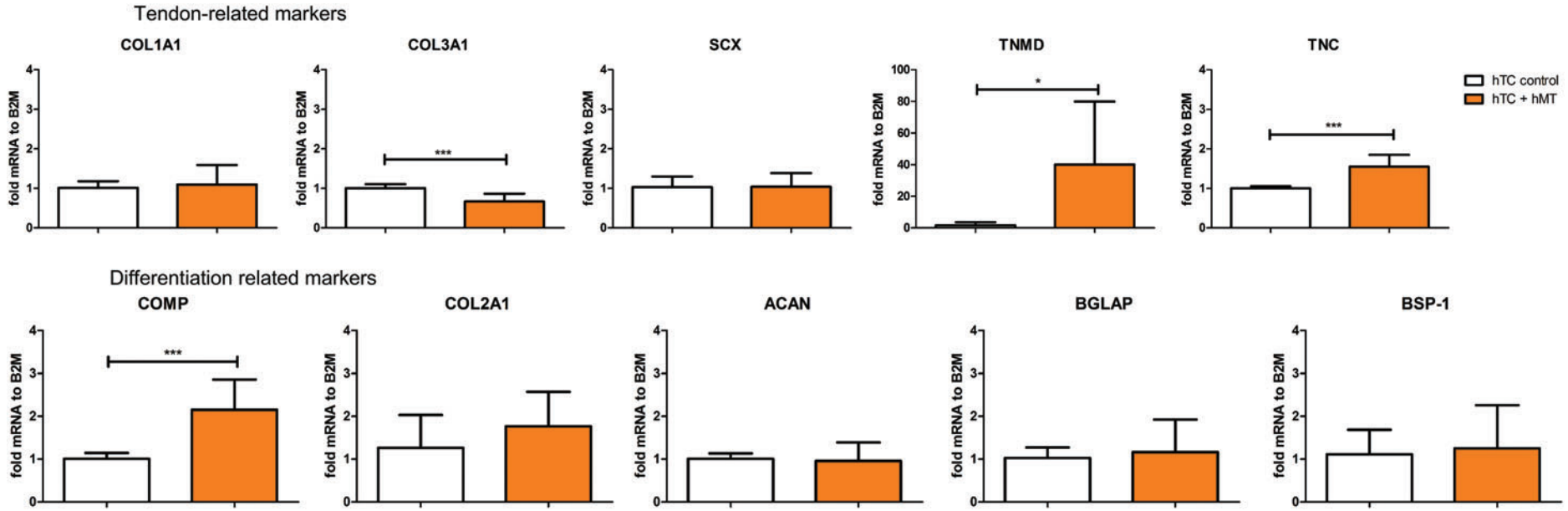

FIG. 5. Gene expression of tendon-, cartilage-, and osteogenic-related markers in hTC when cultured in the presence or absence of muscle-conditioned media. The graphs represent the average in gene expression over three hTC donors. Statistically significant differences were found with $*p < 0.05$ and $***p < 0.001$. Color images available online at www.liebertpub.com/tea

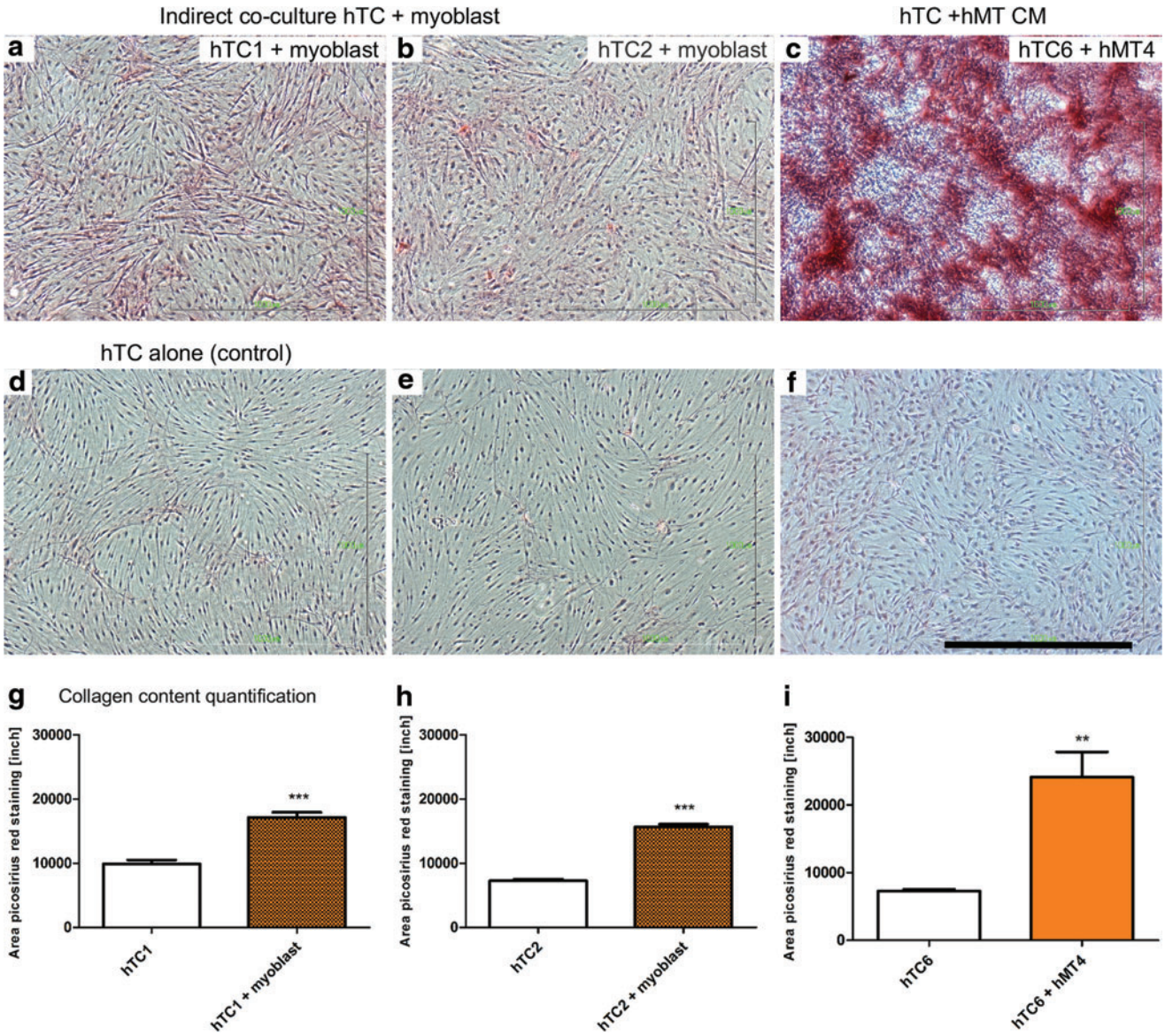

FIG. 6. Picrosirius red staining of hTC indirectly cocultured with myoblasts or exposed to muscle tissue CM. **(a)** hTC1 indirectly cocultured with myoblasts. **(b)** hTC2 indirectly cocultured with myoblasts. **(c)** hTC6 exposed to muscle tissue CM. **(d–f)** hTC1/hTC2/hTC6 cultured alone (negative control). **(g–i)** Quantification of Picrosirius red staining using FIJI software. Statistically significant differences were found with $***p < 0.001$ and $**p < 0.01$. Scale bar represents 1 mm. CM, condition media. Color images available online at www.liebertpub.com/tea

In our attempt to change to a more clinically relevant approach, we examined the influence hMT may have on hTC. Consequently, the remnant hMT removed during preparation of the tendon graft and harvest from a patient undergoing ACL reconstruction[47] offered us the chance to investigate its role in tendon cell commitment and its potential use in accelerating tendon graft remodeling. We found that CM collected from hMT induce, similarly to myoblast coculture, an increase in expression of T/L and cartilage-related markers, which in turn are involved in synthesis and turnover of the ECM. These findings in gene expression were further confirmed in one representative experiment, where an increase in collagen production in hTC exposed to myoblasts or hMT CM was observed. These results are representative as more replicas shall be performed; nevertheless, the data gathered are highly suggestive of the important role muscle-secreted factors have in the healing process. While Murray and Spector have identified the presence of myofibroblasts in the ruptured human ACL and hypothesized that the contractile role of myofibroblasts in the ACL could be responsible for the wrinkling of the ECM and the formation of crimp,[48] Sun *et al.* have shown in a rabbit model that hMT left on tendon graft promotes the intra-articular healing and remodeling of the graft.[49] In this study, we speculate that collection and later stage delivery of hMT CM can improve the remodeling of the ECM for better ligamentization. Since the primary objective is to evaluate the effects of muscle-secreted factors on graft healing, early graft remodeling phase (2–6 weeks postoperation) was selected for administration of the growth factors and examination. At earlier time points (1–2 weeks postoperation), knee swelling and inflammation were still

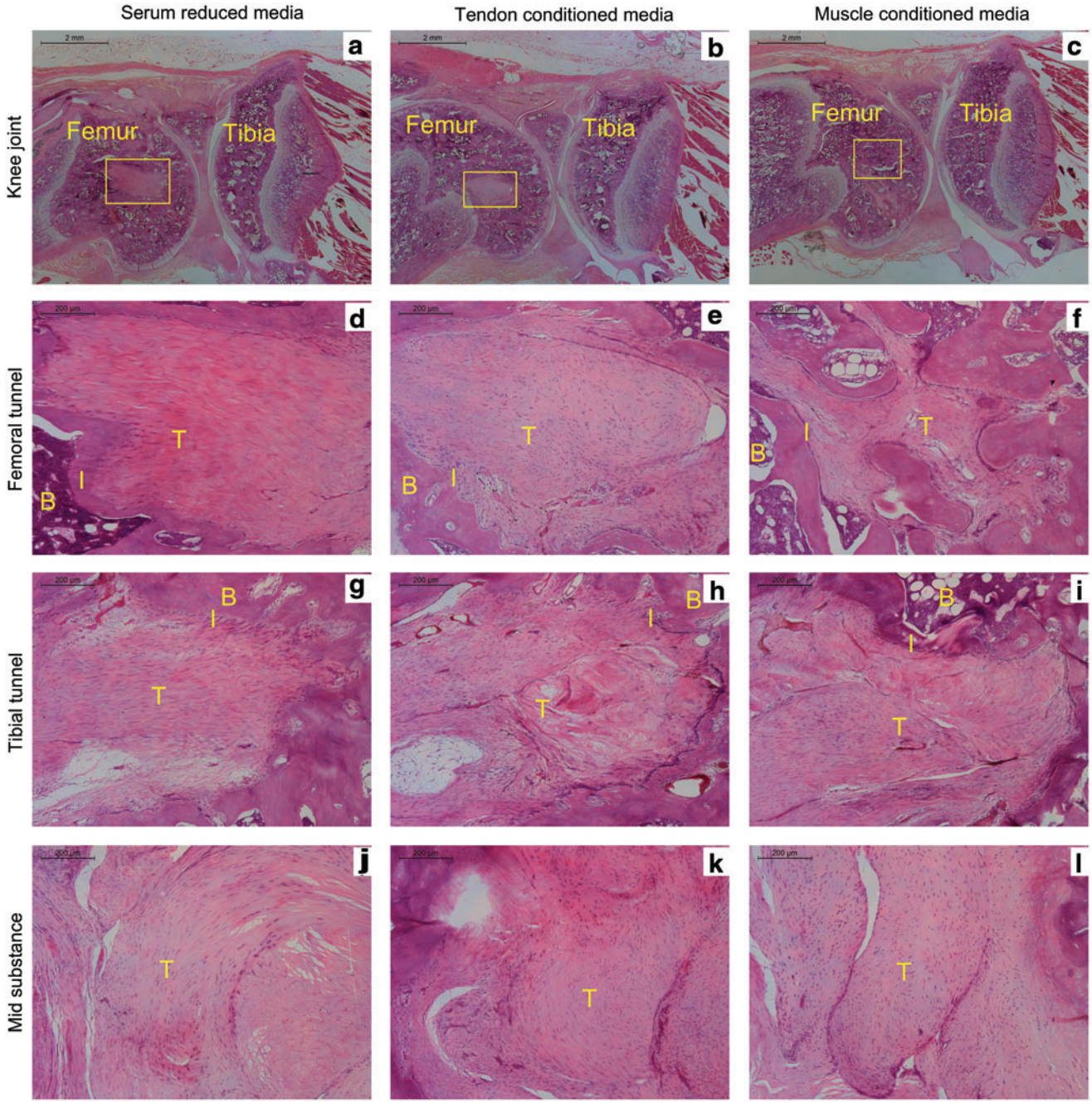

FIG. 7. Histological images showing sagittal views of ACL-reconstructed rat knees at 6 weeks postoperation, treated with basic media, tendon-conditioned media, or muscle-conditioned media. **(d–f)** Magnified image of the tendon graft, marked in *square* of **(a–c)**, respectively. Significant bone tunnel closure is observed in femoral tunnel of muscle-conditioned media group **(c, f)**, but not in other two groups. Sharpey's fiber and fibrocartilage zone present at bone-to-tunnel interface in all groups, as indicated by ''I'' in **(d–i)**. [H&E staining. Optical magnification: 12.5× in **(a–c)**, 100× in **(d–l)**]. B, bone; I, bone–tendon interface; T, tendon graft. ACL, anterior cruciate ligament. Color images available online at www.liebertpub.com/tea

prominent,[17] which is not favorable for growth factor delivery. As tissue regeneration normally starts after the inflammatory phase, it is a better and more feasible choice to start the growth factor supplementation at a longer time point after the inflammatory phase. We used an ACL reconstruction rat model and injected hMT CM, tendon tissue CM, or SRM control into the operated joints of the animals. We showed that femoral tunnel closure was promoted by hMT CM, but tibial tunnel closure was not affected. This difference might be attributed to the different mechanical environments inside femoral and tibial tunnels owing to the relative positions of graft and the tunnels. Moreover, the distribution of bioactive factors in the knee joints on injection of hMT CM may also affect treatment outcomes. A controlled delivery system will be necessary to direct the bioactive factor to the healing site along the tendon graft. In addition, it is worth noticing that the hMT used herein may contain other cell types that can confound the results, and

thus, further analysis is warranted to clarify the contribution of the different cell types and their secretome.

Overall, we showed that myoblasts and muscle tissue-secreted molecules influence hTC commitment and ECM remodeling and are capable of accelerating intra-articular healing in an ACL reconstruction rat model. Consequently, these findings provide preliminary proof that remnant hMT may become a useful tool in accelerating ACL reconstruction healing.

Disclosure Statement

No competing financial interests exist.

References

1. Mall, N.A., Chalmers, P.N., Moric, M., Tanaka, M.J., Cole, B.J., Bach, B.R., Jr., and Paletta, G.A., Jr. Incidence and trends of anterior cruciate ligament reconstruction in the United States. Am J Sports Med **42,** 2363, 2014.
2. Shaerf, D.A., Pastides, P.S., Sarraf, K.M., and Willis-Owen, C.A. Anterior cruciate ligament reconstruction best practice: a review of graft choice. World J Orthop **5,** 23, 2014.
3. Schweitzer, R., Zelzer, E., and Volk, T. Connecting muscles to tendons: tendons and musculoskeletal development in flies and vertebrates. Development **137,** 2807, 2010.
4. Hendriks, J., Riesle, J., and Vanblitterswijk, C.A. Effect of stratified culture compared to confluent culture in monolayer on proliferation and differentiation of human articular chondrocytes. Tissue Eng **12,** 2397, 2006.
5. Ghebes, C.A., Kelder, C., Schot, T., Renard, A.J., Pakvis, D.F., Fernandes, H., and Saris, D.B. Anterior cruciate ligament- and hamstring tendon-derived cells: in vitro differential properties of cells involved in ACL reconstruction. J Tissue Eng Regen Med **11,** 1077, 2017.
6. Mentink, A., Hulsman, M., Groen, N., Licht, R., Dechering, K.J., van der Stok, J., Alves, H.A., Dhert, W.J., van Someren, E.P., Reinders, M.J.T., van Blitterswijk, C.A., and de Boer, J. Predicting the therapeutic efficacy of MSC in bone tissue engineering using the molecular marker CADM1. Biomaterials **34,** 4592, 2013.
7. Le, B.Q., Fernandes, H., Bouten, C.V., Karperien, M., van Blitterswijk, C., and de Boer, J. High-throughput screening assay for the identification of compounds enhancing collagenous extracellular matrix production by ATDC5 cells. Tissue Eng Part C Methods **21,** 726, 2015.
8. Unadkat, H.V., Rewagad, R.R., Hulsman, M., Hulshof, G.F., Truckenmuller, R.K., Stamatialis, D.F., Reinders, M.J., Eijkel, J.C., van den Berg, A., van Blitterswijk, C.A., and de Boer, J. A modular versatile chip carrier for high-throughput screening of cell-biomaterial interactions. J R Soc Interface **10,** 20120753, 2013.
9. Barradas, A.M., Lachmann, K., Hlawacek, G., Frielink, C., Truckenmoller, R., Boerman, O.C., van Gastel, R., Garritsen, H., Thomas, M., Moroni, L., van Blitterswijk, C., and de Boer, J. Surface modifications by gas plasma control osteogenic differentiation of MC3T3-E1 cells. Acta Biomater **8,** 2969, 2012.
10. Gentleman, R.C., Carey, V.J., Bates, D.M., Bolstad, B., Dettling, M., Dudoit, S., Ellis, B., Gautier, L., Ge, Y., Gentry, J., Hornik, K., Hothorn, T., Huber, W., Iacus, S., Irizarry, R., Leisch, F., Li, C., Maechler, M., Rossini, A.J., Sawitzki, G., Smith, C., Smyth, G., Tierney, L., Yang, J.Y., and Zhang, J. Bioconductor: open software development for computational biology and bioinformatics. Genome Biol **5,** R80, 2004.
11. Smyth, G.K. limma: linear models for microarray data. In: Gentleman, R., Carey, V.J., Huber, W., Irizarry, R.A., and Dudoit, S., eds. Bioinformatics and Computational Biology Solutions Using R and Bioconductor. New York: Springer New York, 2005, p. 397.
12. Benjamini, Y., and Hochberg, Y. Controlling the false discovery rate: a practical and powerful approach to multiple testing. J R Stat Soc Series B Methodol **57,** 289, 1995.
13. Huang da, W., Sherman, B.T., and Lempicki, R.A. Systematic and integrative analysis of large gene lists using DAVID bioinformatics resources. Nature protocols **4,** 44, 2009.
14. Huang da, W., Sherman, B.T., and Lempicki, R.A. Bioinformatics enrichment tools: paths toward the comprehensive functional analysis of large gene lists. Nucleic Acids Res **37,** 1, 2009.
15. Fu, S.C., Cheng, W.H., Cheuk, Y.C., Mok, T.Y., Rolf, C.G., Yung, S.H., and Chan, K.M. Effect of graft tensioning on mechanical restoration in a rat model of anterior cruciate ligament reconstruction using free tendon graft. Knee Surg Sports Traumatol Arthrosc **21,** 1226, 2013.
16. Fu, S.C., Cheuk, Y.C., Chiu, W.Y., Yung, S.H., Rolf, C.G., and Chan, K.M. Tripeptide-copper complex GHK-Cu (II) transiently improved healing outcome in a rat model of ACL reconstruction. J Orthop Res **33,** 1024, 2015.
17. Fu, S.-C., Cheng, W.-H., Cheuk, Y.-C., Mok, T.-Y., Rolf, C., Yung, S.-H., and Chan, K.-M. Development of vitamin C irrigation saline to promote graft healing in anterior cruciate ligament reconstruction. J Orthop Transl **1,** 67, 2013.
18. Claes, S., Verdonk, P., Forsyth, R., and Bellemans, J. The ''ligamentization'' process in anterior cruciate ligament reconstruction: what happens to the human graft? A systematic review of the literature. Am J Sports Med **39,** 2476, 2011.
19. Pauzenberger, L., Syre, S., and Schurz, M. ''Ligamentization'' in hamstring tendon grafts after anterior cruciate ligament reconstruction: a systematic review of the literature and a glimpse into the future. Arthroscopy **29,** 1712, 2013.
20. Edom-Vovard, F., and Duprez, D. Signals regulating tendon formation during chick embryonic development. Dev Dyn **229,** 449, 2004.
21. Murchison, N.D., Price, B.A., Conner, D.A., Keene, D.R., Olson, E.N., Tabin, C.J., and Schweitzer, R. Regulation of tendon differentiation by scleraxis distinguishes force-transmitting tendons from muscle-anchoring tendons. Development **134,** 2697, 2007.
22. Schurch, W., Seemayer, T.A., and Gabbiani, G. The myofibroblast: a quarter century after its discovery. Am J Surg Pathol **22,** 141, 1998.
23. Faryniarz, D.A., Chaponnier, C., Gabbiani, G., Yannas, I.V., and Spector, M. Myofibroblasts in the healing lapine medial collateral ligament: possible mechanisms of contraction. J Orthop Res **14,** 228, 1996.
24. Eyre, D.R. Collagens and cartilage matrix homeostasis. Clin Orthop Relat Res **427 Suppl,** S118, 2004.
25. Tchetina, E., Mwale, F., and Poole, A.R. Distinct phases of coordinated early and late gene expression in growth plate chondrocytes in relationship to cell proliferation, matrix assembly, remodeling, and cell differentiation. J Bone Miner Res **18,** 844, 2003.
26. Sahebjam, S., Khokha, R., and Mort, J.S. Increased collagen and aggrecan degradation with age in the joints of Timp3(-/-) mice. Arthritis Rheum **56,** 905, 2007.

27. Ochi, K., Derfoul, A., and Tuan, R.S. A predominantly articular cartilage-associated gene, SCRG1, is induced by glucocorticoid and stimulates chondrogenesis in vitro. Osteoarthritis Cartilage **14,** 30, 2006.
28. Hakala, B.E., White, C., and Recklies, A.D. Human cartilage gp-39, a major secretory product of articular chondrocytes and synovial cells, is a mammalian member of a chitinase protein family. J Biol Chem **268,** 25803, 1993.
29. Chou, C.H., Lee, M.T., Song, I.W., Lu, L.S., Shen, H.C., Lee, C.H., Wu, J.Y., Chen, Y.T., Kraus, V.B., and Wu, C.C. Insights into osteoarthritis progression revealed by analyses of both knee tibiofemoral compartments. Osteoarthritis Cartilage **23,** 571, 2015.
30. Lo, S.H. Tensin. Int J Biochem Cell Biol **36,** 31, 2004.
31. Rockey, D.C., Weymouth, N., and Shi, Z. Smooth muscle alpha actin (Acta2) and myofibroblast function during hepatic wound healing. PLoS one **8,** e77166, 2013.
32. Wittamer, V., Franssen, J.D., Vulcano, M., Mirjolet, J.F., Le Poul, E., Migeotte, I., Brezillon, S., Tyldesley, R., Blanpain, C., Detheux, M., Mantovani, A., Sozzani, S., Vassart, G., Parmentier, M., and Communi, D. Specific recruitment of antigen-presenting cells by chemerin, a novel processed ligand from human inflammatory fluids. J Exp Med **198,** 977, 2003.
33. Kpetemey, M., Dasgupta, S., Rajendiran, S., Das, S., Gibbs, L.D., Shetty, P., Gryczynski, Z., and Vishwanatha, J.K. MIEN1, a novel interactor of Annexin A2, promotes tumor cell migration by enhancing AnxA2 cell surface expression. Mol Cancer **14,** 156, 2015.
34. Nabiev, S.R., Ovsyannikov, D.A., Kopylova, G.V., Shchepkin, D.V., Matyushenko, A.M., Koubassova, N.A., Levitsky, D.I., Tsaturyan, A.K., and Bershitsky, S.Y. Stabilizing the central part of tropomyosin increases the bending stiffness of the thin filament. Biophys J **109,** 373, 2015.
35. Park, C.H., Rha, S.Y., Ahn, J.B., Shin, S.J., Kwon, W.S., Kim, T.S., An, S., Kim, N.K., Yang, W.I., and Chung, H.C. PINCH-2 presents functional copy number variation and suppresses migration of colon cancer cells by paracrine activity. Int J Cancer **136,** 2273, 2015.
36. Pal, S.K., Nguyen, C.T., Morita, K.I., Miki, Y., Kayamori, K., Yamaguchi, A., and Sakamoto, K. THBS1 is induced by TGFB1 in the cancer stroma and promotes invasion of oral squamous cell carcinoma. J Oral Pathol **45,** 730, 2016.
37. Izumi, D., Ishimoto, T., Miyake, K., Sugihara, H., Eto, K., Sawayama, H., Yasuda, T., Kiyozumi, Y., Kaida, T., Kurashige, J., Imamura, Y., Hiyoshi, Y., Iwatsuki, M., Iwagami, S., Baba, Y., Sakamoto, Y., Miyamoto, Y., Yoshida, N., Watanabe, M., Takamori, H., Araki, N., Tan, P., and Baba, H. CXCL12/CXCR4 activation by cancer-associated fibroblasts promotes integrin beta1 clustering and invasiveness in gastric cancer. Int J Cancer **138,** 1207, 2016.
38. Leblanc, R., Lee, S.C., David, M., Bordet, J.C., Norman, D.D., Patil, R., Miller, D., Sahay, D., Ribeiro, J., Clezardin, P., Tigyi, G.J., and Peyruchaud, O. Interaction of platelet-derived autotaxin with tumor integrin alphaVbeta3 controls metastasis of breast cancer cells to bone. Blood **124,** 3141, 2014.
39. Aeffner, F., Woods, P.S., and Davis, I.C. Activation of A1--adenosine receptors promotes leukocyte recruitment to the lung and attenuates acute lung injury in mice infected with influenza A/WSN/33 (H1 N1) virus. J Virol **88,** 10214, 2014.
40. Shan, N., Zhang, X., Xiao, X., Zhang, H., Tong, C., Luo, X., Chen, Y., Liu, X., Yin, N., Deng, Q., and Qi, H. Laminin alpha4 (LAMA4) expression promotes trophoblast cell invasion, migration, and angiogenesis, and is lowered in preeclamptic placentas. Placenta **36,** 809, 2015.
41. Grau, S.J., Trillsch, F., Tonn, J.C., Goldbrunner, R.H., Noessner, E., Nelson, P.J., and von Luettichau, I. Podoplanin increases migration and angiogenesis in malignant glioma. Int J Clin Exp pathol **8,** 8663, 2015.
42. MacDonald, T.J., Brown, K.M., LaFleur, B., Peterson, K., Lawlor, C., Chen, Y., Packer, R.J., Cogen, P., and Stephan, D.A. Expression profiling of medulloblastoma: PDGFRA and the RAS/MAPK pathway as therapeutic targets for metastatic disease. Nat Genet **29,** 143, 2001.
43. Deshmane, S.L., Kremlev, S., Amini, S., and Sawaya, B.E. Monocyte chemoattractant protein-1 (MCP-1): an overview. J Interferon Cytokine Res **29,** 313, 2009.
44. Engsig, M.T., Chen, Q.J., Vu, T.H., Pedersen, A.C., Therkidsen, B., Lund, L.R., Henriksen, K., Lenhard, T., Foged, N.T., Werb, Z., and Delaisse, J.M. Matrix metalloproteinase 9 and vascular endothelial growth factor are essential for osteoclast recruitment into developing long bones. J Cell Biol **151,** 879, 2000.
45. Maghazachi, A.A., Al-Aoukaty, A., and Schall, T.J. CC chemokines induce the generation of killer cells from CD56+ cells. Eur J Immunol **26,** 315, 1996.
46. Lee, W., Aitken, S., Sodek, J., and McCulloch, C.A. Evidence of a direct relationship between neutrophil collagenase activity and periodontal tissue destruction in vivo: role of active enzyme in human periodontitis. J Periodont Res **30,** 23, 1995.
47. Phillips, B.B. Arthroscopy of the lower extremity. In: Canale, S.T., and Beaty, J.H., eds. Campbell's Operative Orthopaedics. Philadelphia: Elsevier Mosby, 2008, p. 2869.
48. Murray, M.M., and Spector, M. Fibroblast distribution in the anteromedial bundle of the human anterior cruciate ligament: the presence of alpha-smooth muscle actin-positive cells. J Orthop Res **17,** 18, 1999.
49. Sun, L., Hou, C., Wu, B., Tian, M., and Zhou, X. Effect of muscle preserved on tendon graft on intra-articular healing in anterior cruciate ligament reconstruction. Knee Surg Sports Traumatol Arthrosc **21,** 1862, 2013.

Address correspondence to:
Daniel B.F. Saris, MD, PhD
Faculty of Science and Technology
Institute of Technical Medicine
University of Twente
P.O. Box 217
Enschede 7500 AE
The Netherlands

E-mail: d.b.f.saris@utwente.nl

Hugo Machado Fernandes, PhD
Stem Cells and Drug Screening Lab
Center for Neurosciences and Cell Biology (CNC)
University of Coimbra
Largo Marquês de Pombal
Coimbra 3004-517
Portugal

E-mail: hugo.fernandes@uc-biotech.pt

Received: December 15, 2016
Accepted: May 10, 2017
Online Publication Date: July 5, 2017